Modeling Dielectric Constant of Semiconductor Nanocrystals

M. Li and H. Li

***Abstract*—A simple and unified model has been established for size- and composition-dependent dielectric constant $\varepsilon(x, D)$ based on a size-dependent melting-temperature model, where x is the fraction of composition, D denotes the diameter of nanoparticles and nanowires, and the thickness of thin films. It demonstrates that depending on the dimension of nanocrystals, $\varepsilon(x, D)$ decreases with different trend as D drops, while $\varepsilon(x, D)$ is a nonlinear function of x. The theoretical prediction agrees approximately with experimental and computer simulation results of semiconductor nanocrystals in single phase or multiphases.**

***Index Terms*—Alloy, component effect, dielectric constant, semiconductor, size effect.**

I. Introduction

LOW-DIMENSIONAL nanocrystals (nanoparticles, nanowires, and thin films) exhibit fascinating physicochemical properties dramatically different from the corresponding bulk counterparts, which has attracted great attention because of potentially immense applications [1]. As one of the most important parameters for physical and optoelectrical characteristics, dielectric constant ε is a quantum that describes how much electric field (flux) is generated per unit charge and has been intensively investigated in both experimental and theoretical methods [2]. It has been recognized that in nanomaterials with the size D, $\varepsilon(D) < \varepsilon(\infty)$ because of the lower screening of confined electrons [3]–[5], where D denotes the diameter of nanoparticles or nanowires, and the thickness of thin films, and ∞ denotes the corresponding bulk crystals. The reduced $\varepsilon(D)$ can enhance the Coulomb interactions among electrons, holes, and ionized shallow impurities in nanodevices, significantly modifying the optical absorption and transport properties [2]. For a more promising application: nanocrystal flash memories, nanocrystal is usually embedded in the gate oxide as a charge storage node, but the inclusion is expected to affect the gate capacitance [6]–[8]. Thus, a basic understanding of dielectric properties is critical for designing devices of desired performance. Size effect on $\varepsilon(D)$ has been verified by recent first-principles calculations and other theoretical investigations [2], [5], [9]. In spite, of great efforts devoted to the achievements of demanded optical properties by tuning the dielectric constant of nanocrystals via changing the size, in particular, down to 2–3 nm, one has to envisage an insurmountable stability problem [10]. To resolve this limit, multiphase alloys have been of special interest because of higher stability [10], as well as the unique superiorities such as high luminescence and the basic optical properties of the corresponding single-phase nanocrystals [11].

Although there were some models to be proposed for the $\varepsilon(D)$ function, the theoretical predictions that were in good consistence with experimental results indispensably relied on some adjustable parameters in these models [2], [12]. This naturally limits the direct use of these models [2], [12]. Moreover, because of few considerations about the composition (x) effect on $\varepsilon(x, D)$ in multiphase alloys, to develop a quantitative model for $\varepsilon(x, D)$ covering both size and composition effects, becomes highly desirable.

In this contribution, based on several known thermodynamic functions, a model without any adjustable parameter, has been developed to predict the $\varepsilon(x, D)$ function. According to this model, $\varepsilon(x, D)$ is demonstrated to decrease with D for different nanocrystals in elements, compounds, and multiphase alloys. Furthermore, $\varepsilon(x, D)$ can also be effectively tuned by selecting proper x for alloys, and the validity is verified by the experimental and computer simulation results, suggesting an effective way to develop their applications in optoelectronic devices.

II. Model

According to the nearly-free-electron approach, $E_{\mathrm{g}} = 2|V_1|$. Here, E_{g} denotes the band gap, which is a major factor determining the electrical conductivity of materials. V_1 is the crystalline field depending on the total number of atoms and interatomic interaction of solids (V) [13]. Generalizing this relationship into nanometer size range, as a first approximation, it can be obtained that

$$\frac{\Delta E_{\mathrm{g}}(D)}{E_{\mathrm{g}}(\infty)} = \left|\frac{\Delta V(D)}{V(\infty)}\right| \tag{1}$$

where shows the difference. Since $V \propto E_{\mathrm{c}}$ [13], where E_{c} is the atomic cohesive energy, there is

$$\left|\frac{\Delta V(D)}{V(\infty)}\right| = \left|\frac{E_{\mathrm{c}}(D) - E_{\mathrm{c}}(\infty)}{E_{\mathrm{c}}(\infty)}\right| = 1 - \frac{E_{\mathrm{c}}(D)}{E_{\mathrm{c}}(\infty)}. \tag{2}$$

Manuscript received September 5, 2011; accepted July 24, 2012. Date of publication August 2, 2012; date of current version September 1, 2012. This work was supported in part by the Natural Science Foundation of Anhui Higher Education Institutions of China under Grant KL2012B159, in part by the Open Foundation of Key Laboratory of Automobile Materials of the Ministry of Educations, Jilin University under Grant 12-450060481289, and in part by the Huaibei Normal University under Grant 700435. The review of this paper was arranged by Associate Editor Y.-H. Cho.

M. Li is with the School of Physics and Electric Information, Huaibei Normal University, Huaibei 235000, China (e-mail: liming2010@chnu.edu.n).

H. Li is with the College of Materials Science and Engineering, Taiyuan University of Technology, Taiyuan 030024, China (e-mail: lihui1012@yahoo.com.cn).

Digital Object Identifier 10.1109/TNANO.2012.2211382

The function of $E_c(D)$ has been given as [14]

$$\frac{E_c(D)}{E_c(\infty)} = \frac{T_m(D)}{T_m(\infty)} = \exp\left[-\frac{2S_{vib}(\infty)}{3R}\frac{1}{D/D_0 - 1}\right] \quad (3)$$

where T_m is the melting temperature, $S_{vib}(\infty)$ is the bulk vibrational melting entropy, and R is the ideal gas constant. For semiconductors, $S_{vib}(\infty) \approx S_m(\infty)$–$R$ is usually employed as a rough approximation and $S_m(\infty)$ denotes the bulk melting entropy [15]. D_0 means a critical diameter at which all atoms of a low-dimensional material are located on its surface. As a function of both dimensionality d and atomic distance h, D_0 is determined by [15]

$$D_0 = 2(3-d)h \quad (4)$$

where $d = 0$, 1, and 2 for nanoparticles, nanowires, and thin films, respectively. It should be mentioned that except for free nanoparticles with $d = 0$, $d = 1$ is assumed for nanoparticles deposited on substrates with the shape of island or disk [15].

The dielectric constant originates from electronic polarization or electron transition from the lower valence band to the upper conduction band. This process is subject to the selection rule of energy and momentum conservation, which determines the optical response of semiconductors and reflects how strongly the valence electrons couple with the excited conduction electrons [2]. Therefore, the ε of a semiconductor is directly related to its E_g at room temperature. According to (1)–(3) an approximate relation of $\chi(\infty) \propto E_g^{-2}$ [2], the size dependent electron polarization coefficient $\chi(D)$ can be given by $[\chi(D)/\chi(\infty)] = \{2 - [T_m(D)/T_m(\infty)]\}^{-2}$. Extending the relationship of $\varepsilon = \chi + 1$ into nanoscale gives rise to the $\varepsilon(D)$ function, namely

$$\frac{\varepsilon(D) - 1}{\varepsilon(\infty) - 1} = \left\{2 - \exp\left[-\frac{2S_{vib}(\infty)}{3R}\frac{1}{D/D_0 - 1}\right]\right\}^{-2}. \quad (5)$$

In order to clear the contribution induced from composition variation, $\varepsilon(x, \infty)$ of ternary alloys or pseudobinary solutions with regular solution is introduced [16]

$$\varepsilon(x,\infty) = x\varepsilon(0,\infty) + (1-x)\varepsilon(1,\infty) + \Omega(x,\infty)x(1-x) \quad (6)$$

where 0 and 1 separately represent the components in a binary alloy, x denotes the molar ratio of component "0" in the alloy, and $\Omega(x, \infty)$ is the bowing parameter of bulk crystals, which results in the bowing behavior of $\varepsilon(x, \infty)$.

In a similar way as expressed in (6), it is easy to obtain the $\varepsilon(x, D)$ function for nanocrystals

$$\varepsilon(x,D) = x\varepsilon(0,D) + (1-x)\varepsilon(1,D) + \Omega(x,D)x(1-x) \quad (7)$$

with $\Omega(x, D)$ given by [10]

$$\frac{\Omega(x,D)}{\Omega(x,8)} = \frac{1 - 2D_0(x)}{D} \quad (8)$$

where $D_0(x)$ is critical diameter of alloying nanocrystals. $D_0(x) = 2(3–d)h(x)$ [10]. It is well known that Vegard's law is an approximate empirical rule which holds that a linear relation exists, at constant temperature, between the crystal lattice constant of an alloy and the concentrations of the constituent elements [17]. Thus, $h(x)$ can be expressed as

$$h(x) = xh(0) + (1-x)h(1) \quad (9)$$

with $h(0)$ and $h(1)$ denoting the atomic distance of bulk crystals with an assumption that h is almost a size-independent amount [10].

Thus, substituting (8) into (7) gives rise to the expression of $\varepsilon(x, D)$ function of alloying nanocrystals

$$\varepsilon(x,D) = x\varepsilon(0,D) + (1-x)\varepsilon(1,D) + \left(\frac{1-2D_0(x)}{D}\right)\Omega(x,\infty)x(1-x). \quad (10)$$

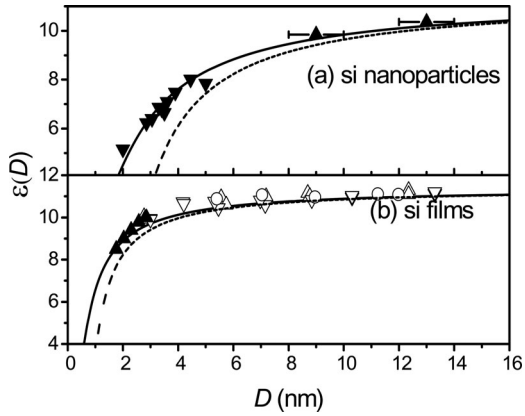

Fig. 1. $\varepsilon(D)$ function of Si nanoparticles and thin films. The solid lines denote the model predictions in terms of (5) and the dashed lines denote the Tsu's model predictions [12]. (a) Symbols (▼) [2] and (▲) [9] are corresponding computer simulantion results of Si nanoparticles. (b) Symbols (▲) [3] and (△), (○), and (▽) [4] denote the corresponding experimental results of Si thin films.

TABLE I
RELEVANT DATA USED IN THE CALCULATIONS OF (5) AND (10), WHERE $S_{vib}(\infty)$ IS IN J·(g-atom)$^{-1}$·K^{-1}, a IS IN nm AND h IS IN nm

	ε(∞)	$S_{vib}(\infty)$	a [23]	h [b]
Si	11.4 [2]	6.72 [24]	0.543	0.235
CdS	8.7 [25]	6.18 [a]	0.582	0.252
CdSe	9.7 [25]	6.59 [a]	0.608	0.263
CdTe	10.2 [25]	12.06 [a]	0.648	0.281
ZnS	9.6 [25]	2.19 [a]	0.541	0.234
ZnSe	8.6 [25]	6.81 [a]	0.567	0.245
InP	12.5 [25]	15.63 [a]	0.586	0.254
InAs	15.2 [25]	10.56 [24]	0.606	0.262

[a] $S_{vib}(\infty) = S_m(\infty)$–$R$ [15] with $S_m(\infty)$ = 16.628 J·g-atom^{-1}K^{-1} [24], 14.91 J·g-atom^{-1}K^{-1} [24], 20.37 J·g-atom^{-1}K^{-1} [24], 10.5 J·g-atom^{-1}K^{-1} [24], 31.5 J·g-atom^{-1}K^{-1} [24] and 23.94 J·g-atom^{-1}K^{-1} [24] for CdS, CdSe, CdTe, ZnS, ZnSe and InP respectively.
[b] $h = \sqrt{3}\,a/4$ for the zinc blende structure [10] and a is lattice parameter.

III. RESULTS AND DISCUSSION

Fig. 1 shows the plot comparing the model predictions according to (5) (solid lines) with Tsu's theoretical evidence (dashed lines) as well as experimental and theoretical results for $\varepsilon(D)$ of Si nanoparticles and thin films. The parameters utilized in the calculation of (5) are listed in Table I. As we can see, a general trend is that $\varepsilon(D)$ decreases with dropping D as a result of increasing number of surface atoms or surface/volume ratio. The

model prediction is consistent with experimental measurements especially for nanoparticles and thin films with D smaller than 10 and 6 nm, respectively. While $\varepsilon(D)$ approaches to bulk value as $D > 10$ nm. Thus, the surface atoms become prominent in determining the properties of nanocrystals due to their distinct physical characteristics comparing with that of interior atoms. Wang and Zunger proposed that the changes of the dielectric constant are due to the surface of the quantum dot, not the overall size of the dot [5], [9] and Delerue *et al*. thought that dielectric suppression is due to the breaking of surface polarizable bonds [3], which supports the earlier findings of Wang and Zunger. It has been found that as the size of nanocrystals decreases, the lattice contracts and cohesive energy decreases [2]. Although lattice contraction leads to the increasing of single-bond energy, the lower coordination number of surface atoms (existing of breaking bonds at surface) results in the decreasing cohesive energy of nanocrystals with the increasing surface atoms. As the result, coordination-imperfection (cohesive energy decreasing) induced local quantum entrapment perturbs the Hamiltonian that determines the band gap (band-gap expansion) and hence, the process of electron polarization consequently [18]. According to the above analysis, it is reasonable that $\varepsilon(D)$ decreases with dropping D according to the approximate relationship between dielectric constant and band gap. In contrast, as we can see in Fig. 1, Tsu's model is consistent with experimental results or (5) only when $D > 10$ nm. This is due to the limited condition $E_g(D)/E_g(\infty) < 0.5$ [12] although the value of $\Delta E_g(D)/E_g(\infty)$ can be larger than 0.5 for nanocrystals in several nanometers [2]. Compared with Tsu's model, our predictions are in good agreement with the experimental and computer simulation results for Si nanoparticles and thin films in full-size range. Similar results can be found in Fig. 2 for II–VI and III–V semiconductors, in which the good agreement between model predictions and experimental results further verify the validity of model.

The composition effect on $\varepsilon(x, D)$ of nanocrystal alloys in terms of (10) is shown in Fig. 3 and Table II, compared with experimental evidences. On one hand, for a fixed x, $\varepsilon(x, D)$ has a downward shift with D decreasing as that in Figs. 1 and 2. On the other hand, $\varepsilon(x, D)$ shows a shift from an almost linear function to a nonlinear one with the increase of D, exhibiting a bowing behavior. This is determined by the third term $[\Omega(x, D)]$ in (10). For binary alloys with the components in the same group, $h(x)$ is less dependent on composition according to (9) because they have almost similar lattice constants. For simplicity, $D_0(x)$ is assumed to be x-independent. Therefore, $\Omega(x, D) \to 0$ according to (8) with $D \to 2D_0(x)$, leading to a linear characteristic function of $\varepsilon(x, D)$, as shown in Fig. 3 for $CdTe_xSe_{1-x}$ with 4.9 nm. It suggests that when $D \to 2D_0(x)$, $\varepsilon(x, D)$ also can be determined by Végard′s law even if we do not know the value of $\Omega(x,\infty)$. However, for $D = 14$ nm, $\varepsilon(x, D)$ shows a nonlinear relationship with x changing because $\Omega(x, D)$ increases and bowing behavior is obvious with D increasing. When D is increased to larger size, for example, $D = 40$ nm and $D = 50$ nm, size effect on $\varepsilon(x, D)$ is very weak and $\Omega(x, D)$ approaches the to bulk value, where the difference between $\varepsilon(x,40)$ and $\varepsilon(x,50)$ is small and $\varepsilon(x, D)$ can

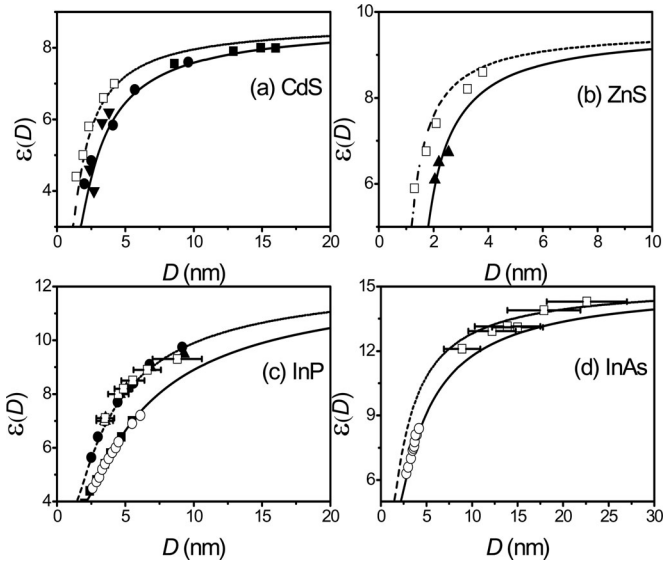

Fig. 2. $\varepsilon(D)$ function of semiconductor compounds in terms of (5). Solid lines denote $\varepsilon(D)$ of nanoparticles and dashed lines denote it of nanowires. The symbols are experimental results. (a) CdS: (▼) [25], (■) [29] and (•) [30] for nanoparticles, and (□) [25] for nanowires. (b) ZnS: (▲) [31] for nanoparticles and (□) [25] for nanowires. (c) InP: (○) and (■) [32] for nanoparticles and (•), (□), and (▲) [32] for nanowires. (d) InAs: (○) [33] for nanoparticles, and (□) [34] for nanowires.

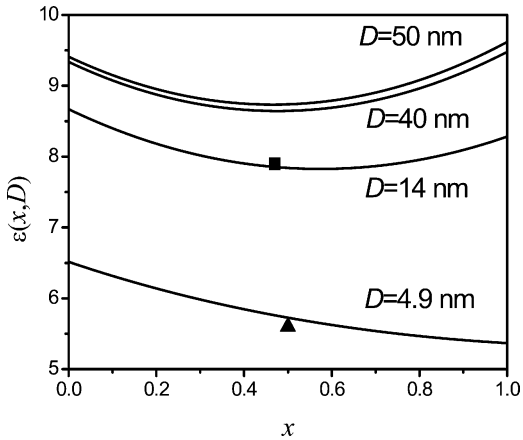

Fig. 3. $\varepsilon(x, D)$ function of $CdTe_xSe_{1-x}$ nanocrystal alloys in terms of (10) (solid lines) and experimental results (■ and ▲ [22]). $\Omega(x, \infty) = -3.32$ [35].

be determined by the bulk value. Similar results for $\varepsilon(x, D)$ of $Zn_xCd_{1-x}Se$, $Cd_xZn_{1-x}S$, and CdS_xSe_{1-x} nanoparticles can be found in Table II and the deviations are less than 5% between calculated and experimental results, which demonstrates that the model can adequately (and quantitatively) describe $\varepsilon(x, D)$ as a function of both composition and size. It is worth mentioning that, (10) is essentially suitable for alloying nanoparticles with free surface or supported by a passivated substrate where there is a weak chemical interaction between the crystal and the substrate [19]–[22]. On the other hand for nanocrystals fabricated by vapor phase deposition methods [10], nanoparticles on substrates have incoherent, semicoherent, or coherent interface, which may induce different tendency like the phenomena of supercooling and superheating observed for nanocrystals with

TABLE II
COMPARISONS OF $\varepsilon(x, D)$ BETWEEN MODEL PREDICTION IN TERMS OF (10) AND THE CORRESPONDING EXPERIMENTAL RESULTS OF TERNARY ALLOYS, WHERE D IS IN nm

	$\Omega(x, \infty)$	x	D	$\varepsilon(x,D)$		% Error (with exp.)
				This work	Exp.	
$Zn_xCd_{1-x}Se$	-1.99 [26]	0.28	5.8	6.87	6.82 [19]	0.73
		0.44	6.3	6.87	6.79 [19]	1.18
		0.55	6.8	6.91	6.80 [19]	1.62
		0.67	7.5	7.00	6.82 [19]	2.63
$Cd_xZn_{1-x}S$	-0.563 [27]	0.25	9	8.60	8.75 [20]	1.71
		0.75	9	7.77	7.80 [20]	0.38
CdS_xSe_{1-x}	-0.563 [28]	0.36	2.8	4.84	5.07 [21]	4.54
		0.43	2.8	4.83	5.05 [21]	4.36
		0.60	3.1	5.16	5.39 [21]	4.27
		0.64	3.1	5.15	5.19 [21]	0.77
		0.2	3.6	5.80	5.75 [21]	0.87
		0.41	3.6	5.70	5.64 [21]	1.06
		0.26	4.3	6.31	6.41 [21]	1.56
		0.39	4.3	6.23	6.01 [21]	3.66
		0.82	4.3	6.08	5.90 [21]	3.05
		0.2	5.8	7.09	7.32 [21]	3.14
		0.75	5.8	6.79	6.96 [21]	2.44

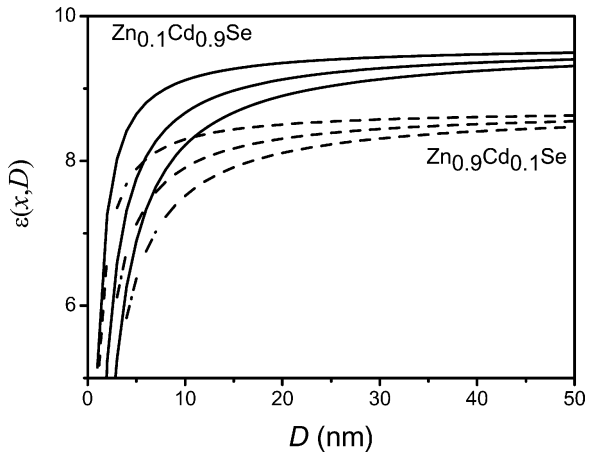

Fig. 4. $\varepsilon(x, D)$ function of $Zn_xCd_{1-x}Se$ with the fixed composition ($x = 0.1$ or 0.9) in terms of (10).

different interface [14]. The interface effect will be considered in further works.

Fig. 4 shows the size-dependent dielectric constant of $Zn_xCd_{1-x}Se$ with the fixed composition ($x = 0.1$ or 0.9) for thin films, nanowires, and nanoparticles, respectively, according to (10). The solid lines are for $x = 0.1$ and the dash lines are for $x = 0.9$. From the top down, the three lines represent $\varepsilon(x, D)$ for thin films, nanowires, and nanoparticles, respectively. An obvious increase in $\varepsilon(x, D)$ is observed in the size range of $D <$10 nm, while $\varepsilon(x, D)$ changes slowly as $D >$ 10 nm. For $Zn_xCd_{1-x}Se$ with different x, the difference of $\varepsilon(x, D)$ for nanocrystals with the same dimensionality is negligible in small size ($D <$ 5 nm), and then becomes obvious when the size becomes larger ($D >$ 5 nm). It indicated that the size effect is evident only when the size is just several nanometers, and the composition effect on $\varepsilon(x, D)$ is obvious for larger size ($D >$ 5 nm). Furthermore, the change of $\varepsilon(x, D)$ of nanowires is weaker than that of nanoparticles and stronger than thin films. These differences should be attributed to the different surface/volume ratios of $A/V = 6/D$, $4/D$, and $2/D$ for nanoparticles, quasi-dimensional nanoparticles or nanowires, and thin films with $d = 0$, 1, and 2, respectively. The result shows that both size and composition can tune the dielectric constant of alloying nanocrystals. In order to meet the desired dielectric constant, applying alloying nanocrystals is a better way by tuning the composition and size compared to elements and compounds just by tuning size, which suggests an effective approach to develop the applications of nanomaterials in optoelectronic devices.

IV. CONCLUSION

In summary, a thermodynamically quantitative model has been developed to calculate $\varepsilon(x, D)$ functions of semiconductor elements, compounds, and alloys. $\varepsilon(x, D)$ decreases with decreasing D, and shows a bowing behavior as a function of x, depending on the size of nanocrystal. Furthermore, the size effect on dielectric constant of nanowires is weaker than that of nanoparticles and stronger than thin films due to the difference surface/volume ratio. Consistency between the model prediction with experimental and computer simulation results confirmed that the model could be expected to be a valid approach to analyze the optical properties of nanomaterials, which will accelerate the applications of nanomaterials in optoelectronic devices.

REFERENCES

[1] L. T. Canham, "Silicon quantum wire array fabrication by electrochemical and chemical dissolution of wafers," *Appl. Phys. Lett.*, vol. 57, pp. 1046–1048, Sep. 1990.

[2] C. Q. Sun, X. W. Sun, B. K. Tay, S. P. Lau, H. T. Huang, and S. Li, "Dielectric suppression and its effect on photoabsorption of nanometric

semiconductors," *J. Phys. D: Appl. Phys.*, vol. 34, pp. 2359–2362, Aug. 2001.

[3] C. Delerue, M. Lannoo, and G. Allan, "Concept of dielectric constant for nanosized systems," *Phys. Rev. B*, vol. 68, pp. 115411-1–115411-4, Sep. 2003.

[4] H. G. Yoo and P. M. Fauchet, "Dielectric constant reduction in silicon nanostructures," *Phys. Rev. B*, vol. 77, pp. 115355-1–115355-5, Mar. 2008.

[5] L. W. Wang and A. Zunger, "Pseudopotential calculations of nanoscale CdSe quantum dots," *Phys. Rev. B*, vol. 53, pp. 9579–9582, Apr. 1996.

[6] J. S. de Sousa, R. Peibst, M. Erenburg, E. Bugiel, G. Farias, J. P. Leburton, and K. R. Hofmann, "Single-electron charging and discharging analyses in Ge-nanocrystal memories," *IEEE Trans. Electron Devices*, vol. 58, no. 2, pp. 376–383, Feb. 2011.

[7] R. Peibst, J. S. de Sousa, and K. R. Hofmann, "Determination of the Ge-nanocrystal/SiO_2 matrix interface trap density from the small signal response of charge stored in the nanocrystals," *Phys. Rev. B*, vol. 82, pp. 195415-1–195415-12, Nov. 2010.

[8] S. Tiwari, F. Rana, H. Hanafi, A. Hartstein, E. F. Crabbe, and K. Chan, "A silicon nanocrystals based memory," *Appl. Phys. Lett.*, vol. 68, pp. 1377–1379, Dec. 1996.

[9] L. W. Wang and A. Zunger, "Dielectric constants of silicon quantum dots," *Phy. Rev. Lett.*, vol. 73, pp. 1039–1042, Aug. 1994.

[10] Y. F. Zhu, X. Y. Lang, and Q. Jiang, "The effect of alloying on the bandgap energy of nanoscaled semiconductor alloys," *Adv. Funct. Mater.*, vol. 18, pp. 1422–1429, Apr. 2008.

[11] E. Sakalauskas, B. Reuters, L. R. Khoshroo, H. Kalisch, M. Heuken, A. Vescan, M. Röppischer, C. Cobet, G. Gobsch, and R. Goldhahn, "Dielectric function and optical properties of quaternary AlInGaN alloys," *J. Appl. Phys.*, vol. 110, pp. 013102-1–013102-9, Jul. 2011.

[12] R. Tsu and D. Babić, "Doping of a quantum dot," *Appl. Phys. Lett.*, vol. 64, pp. 1806–1808, Jun. 1994.

[13] X. Y. Lang, W. T. Zheng, and Q. Jiang, "Finite-size effect on band structure and photoluminescence of semiconductor nanocrystals," *IEEE Trans. Nanotechnol.*, vol. 7, no. 1, pp. 5–9, Jan. 2008.

[14] Q. Jiang, Z. Zhang, and J. C. Li, "Melting thermodynamics of nanocrystals embedded in a matrix," *Acta Mater.*, vol. 48, pp. 4791–4795, Dec. 2000.

[15] Z. Zhang, M. Zhao, and Q. Jiang, "Melting temperatures of semiconductor nanocrystals in the mesoscopic size range," *Semicond. Sci. Technol.*, vol. 16, pp. L33–L35, 2001.

[16] D. Richardson and R. Hill, "Dielectric function variations in ternary zinc compound semiconductor alloy systems," *J. Phys. C: Solid State Phys.*, vol. 6, pp. L131–L134, Mar. 1973.

[17] L. Vegard, "Die konstitution der mischkristalle und die raumfüllung der atome," *Zeitschrift für Physik A Hadrons Nuclei*, vol. 5, pp. 17–26, Dec. 1921.

[18] E. S. M. Goh, T. P. Chen, H. Y. Yang, Y. Liu, and C. Q. Sun, "Size-suppressed dielectrics of Ge nanocrystals: Skin-deep quantum entrapment," *Nanoscale*, vol. 4, pp. 1308–1311, Jan. 2012.

[19] X. Zhong, M. Han, Z. Dong, T. J. White, and W. Knoll, "Composition-tunable $Zn_x Cd_{1-x} Se$ nanocrystals with high luminescence and stability," *J. Amer. Chem. Soc.*, vol. 125, pp. 8589–8594, Jun. 2003.

[20] D. V. Petrov, B. S. Santos, G. A. L. Pereira, and C. de Mello Donegá, "Size and band-gap dependences of the first hyperpolarizability of $Cd_x Zn_{1-x} S$ nanocrystals," *J. Phys. Chem. B*, vol. 106, pp. 5325–5334, May 2002.

[21] L. A. Swafford, L. A. Weigand, M. J. Bowers, J. R. McBride, J. L. Rapaport, T. L. Watt, S. K. Dixit, L. C. Feldman, and S. J. Rosenthal, "Homogeneously alloyed $CdS_x Se_{1-x}$ nanocrystals: Synthesis, characterization, and composition/size-dependent band gap," *J. Amer. Chem. Soc.*, vol. 128, pp. 12299–12306, Sep. 2006.

[22] Y. C. Li, H. Z. Zhong, R. Li, Y. Zhou, C. H. Yang, and Y. F. Li, "High-yield fabrication and electrochemical characterization of tetrapodal CdSe, CdTe, and $CdSe_x Te_{1-x}$ nanocrystals," *Adv. Funct. Mater.*, vol. 16, pp. 1705–1716, Jul. 2006.

[23] D. W. Palmer. (2003). [Online]. Available: http://www.semiconductors.co.uk/

[24] A. R. Regel and V. M. Glazov, "Entropy of melting of semiconductors," *Semiconductors*, vol. 29, pp. 405–417, May 1995.

[25] J. Li and L. W. Wang, "Band-structure-corrected local density approximation study of semiconductor quantum dots and wires," *Phys. Rev. B*, vol. 72, pp. 125325-1–125325-15, Sep. 2005.

[26] K. Bouamama, P. Djemia, N. Lebga, and K. Kassali, "Ab initio calculation of the elastic properties and the lattice dynamics of the $Zn_x Cd_{1-x} Se$ alloy," *Semicond. Sci. Technol.*, vol. 24, pp. 045005-1–045005-5, Apr. 2009.

[27] A. M. Salem, "Structure, refractive-index dispersion and the optical absorption edge of chemically deposited $Zn_x Cd_{(1-x)} S$ thin films," *Appl. Phys. A: Mater. Sci. Process.*, vol. 74, pp. 205–211, Jun. 2002.

[28] S. Nomura and T. Kobayashi, "Nonparabolicity of the conduction band in CdSe and $CdS_x Se_{1-x}$ semiconductor microcrystallites," *Solid State Commun.*, vol. 78, pp. 677–680, May 1991.

[29] D. S. Chuu and C. M. Dai, "Quantum size effects in CdS thin films," *Phys. Rev. B*, vol. 45, pp. 11805–11810, May 1992.

[30] T. Torimoto, H. Kontani, Y. Shibutani, S. Kuwabata, T. Sakata, H. Mori, and H. Yoneyama, "Characterization of ultrasmall CdS nanoparticles prepared by the size-selective photoetching technique," *J. Phys. Chem. B*, vol. 105, pp. 6838–6845, Jun. 2001.

[31] R. Rossetti, R. Hull, J. M. Gibson, and L. E. Brus, "Excited electronic states and optical spectra of ZnS and CdS crystallites in the $\sim$15 to 50 Å size range: Evolution from molecular too bulk semiconducting properties," *J. Chem. Phys.*, vol. 82, pp. 552–559, Jan. 1985.

[32] H. Yu, J. Li, R. A. Loomis, L.-W. Wang, and W. E. Buhro, "Two- versus three-dimensional quantum confinement in indium phosphide wires and dots," *Nat. Mater.*, vol. 2, pp. 517–520, Jul. 2003.

[33] A. A. Guzelian, U. Banin, A. V. Kadavanich, X. Peng, and A. P. Alivisatos, "Colloidal chemical synthesis and characterization of InAs nanocrystal quantum dots," *Appl. Phys. Lett.*, vol. 69, pp. 1432–1434, Sep. 1996.

[34] S. Kan, T. Mokari, E. Rothenberg, and U. Banin, "Synthesis and size-dependent properties of zinc-blended semiconductor quantum rods," *Nature Mater.*, vol. 2, pp. 155–158, Feb. 2003.

[35] L. Hannachi and N. Bouarissa, "Electronic structure and optical properties of $CdSe_x Te_{1-x}$ mixed crystals," *Superlattices Microst.*, vol. 44, pp. 794–801, Oct. 2008.

Authors' photographs and biographies not available at the time of publication.